Electronic Supplementary Material (ESI) for Lab on a Chip.
This journal is © The Royal Society of Chemistry 2017

Supplementary Information

Rapid contrast matching by microflow SANS

Marco Adamo,[a,b] Andreas S. Poulos,[a] Ruhina M. Miller,[a] Carlos G. Lopez,[ac] Anne Martel,[b] Lionel Porcar,[b] and João T. Cabral[a]*

[a]Department of Chemical Engineering, Imperial College London, London SW7 2AZ, United Kingdom.

[b]Institute Laue-Langevin, 71 avenue des Martyrs, 38000 Grenoble, France

[c]Present address: Institute of Physical Chemistry, RWTH Aachen University, Landoltweg 2,

52056 Aachen, Germany.

E-mail: j.cabral@imperial.ac.uk

I. SANS data reduction and calibration in microfluidic cell with over-illuminated microchannels

SANS neutron cells for liquid samples are typically quartz cuvettes (Hellma) and the neutron beam traverses two quartz windows and the sample, in a 'sandwich' arrangement. The empty cell subtraction and data calibration is straightforward and is generally carried out with a standard program (e.g. GRASP at ILL). In this work, we have resorted to employ a beam footprint which is considerably larger that the width of a microchannel and therefore over-illuminates approximately 16-18 channels, in order to attain adequate statistics with a SANS acquisition time of 5-20 s per spectrum. As illustrated in Scheme 1, the scattering volume in the *xy* plane comprises two elements: the channels filled with the sample and the microdevice material (glass, or fused silica, in this case). The total illuminated area is defined as A_{tot}, and is typically 1 cm^2, obtain by a diaphragm of 1cm x 1cm. The fraction of illuminated glass is $A_{glass}/A_{tot}\equiv\varphi$, and thus the area fraction of illuminated channels reads $A_{channel}/A_{tot}\equiv 1-\varphi$, since $A_{channel}+A_{glass}=A_{tot}$. In the z-direction, both φ and $1-\varphi$ areas contain glass above and below, as shown in cross-sectional Scheme 2.

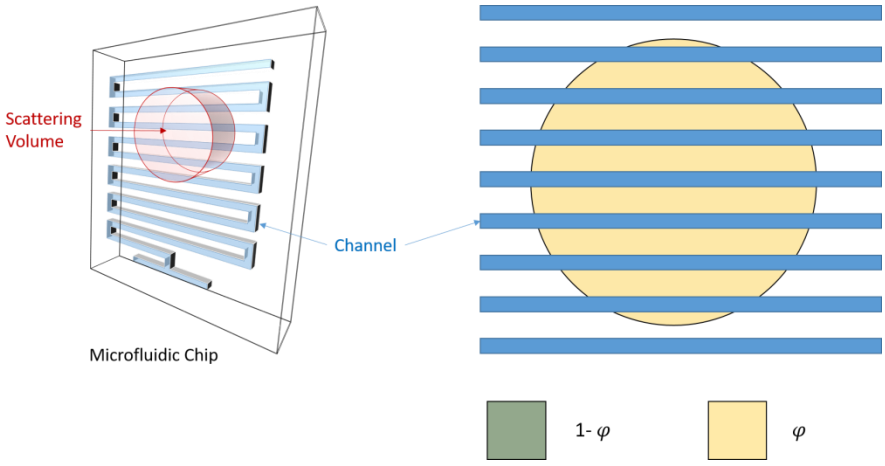

Scheme S1: Illuminated volume (red) of a microfluidic device with over-illumination of several microchannels. The channels (blue) represent a fraction 1-φ of the illuminated area, while the glass covers the remaining φ.

Taking *w* as the channel width, *s* as the inter-channel spacing, and $f=w+s$ as spacing between channel centres, the illuminated sample area fraction is $1-\varphi = w/f$, and the area fraction due to glass-only is $\varphi = s/f$. This estimation is correct provided that an exact (or a large) number of channels is measured; otherwise, a detailed fractional estimation must be obtained experimentally by an explicit measure of the illuminated area. For the

specific 3-port 250 µl microreactor (Dolomite), w = 400 µm and $f = s+w$ = 600 µm, and therefore φ = 200/600 = 0.3(3) and $1-\varphi$ =0.6(6). The channel height h = 250 µm, and the total thickness of the device is t = 4.63 mm. This procedure, however, applies generally to the data analysis from microdevices fabricated by frontal photopolymerisation (FPP) reported earlier [1-4].

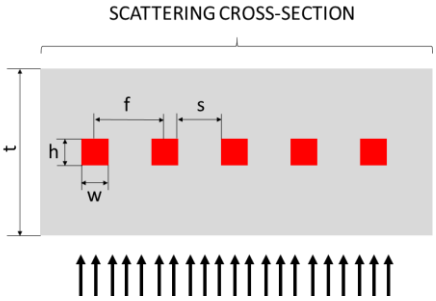

Scheme S2: Cross-section of a representative microfluidic device, where w *is the channel width,* s *is the inter-channel spacing,* f=w+s *the spacing between channel centres,* h *is the channel height and* t *the total thickness of the device. The sample is confined in well-defined channels (red).*

From a small angle scattering (and/or, low h), the layout in Scheme 2 is equivalent to the simpler layout in Scheme 3, provided that φ and $1-\varphi$ are kept constant:

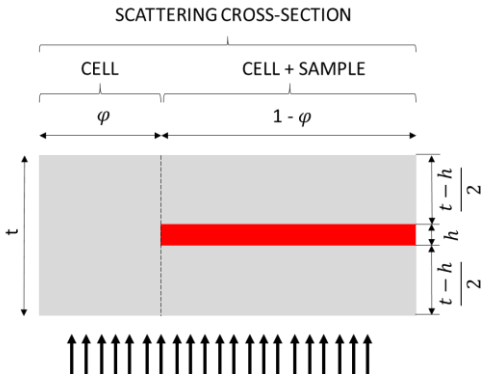

Scheme S3: Equivalent cross section of the microfluidic layout of Scheme 2, comprising a solid cell block and the equivalent of a cell+sample 'sandwich' standard cell of uniform sample thickness h (analogous to a Hellma cell).

SANS data reduction and calibration require both measurements of neutron beam transmission T and scattering I, from a given sample thickness. The experimentally measured transmission of the *empty cell* is T_{empty}=0.91. Experimentally, the measured transmission is the ratio forward neutron intensity measured during a given time interval:

$$T_{empty} \equiv \frac{Empty\ cell}{Empty\ beam} \qquad (1)$$

Following Scheme S3, the theoretical transmission is given by:

$$T_{empty} = \varphi e^{-\mu_{glass} t} + (1-\varphi) e^{-\mu_{glass}(t-h)} \qquad (2)$$

Since all parameters φ, t, and h are known, the glass absorption is readily determined to be μ_{glass} = 0.021 mm^{-1}.

The calibrated [cm^{-1}] scattering signal of the empty cell is given by the sum of the scattering of the bulk glass and that of the empty 'sandwich' glass + air, as:

$$I^{empty} = K_{abs}\left[\varphi \frac{I^{t}}{t T_{glass}^{t}} + (1-\varphi)\frac{I^{t-h}}{(t-h)\, T_{glass}^{t-h}}\right] \qquad (3)$$

where K_{abs} is a calibration factor, measured by the direct beam flux.[1]

Following scheme 3, the sample *transmission* in the microfluidic device, is related to the overall measured transmission of the device + samples, according to:

$$T^{measured} = \varphi e^{-\mu_{glass} t} + (1\text{-}\varphi) e^{-\mu_{glass}(t-h)} e^{-\mu_{sample} h} \qquad (5)$$

where

- $e^{-\mu_{glass} t}$ is the transmission of the solid glass (T^{glass})
- $e^{-\mu_{glass}(t-h)}$ is the transmission of the glass above and below the sample
- $e^{-\mu_{sample} h}$ is the transmission of the sample

Similarly, the total *scattering intensity* is given by the sum of scattering of the solid glass and a term arising from the "sample/glass sandwich" (glass+sample+glass, termed SG_ sandwich):

$$I^{total} = \varphi I^{solid\ glass} + (1-\varphi) I^{\text{SG\_ sandwich}} \qquad (6)$$

In order to calculate the scattering intensity of the sample/glass sandwich, the solid glass contribution must be removed:

$$I^{\text{SG\_ sandwich}} = \frac{I^{total} - \varphi I^{solid\ glass}}{1-\varphi} \qquad (7)$$

It is then possible to treat the problem as a standard data reduction:

$$I^{sample} = K_{abs} \left(\frac{I^{\text{SG\_ sandwich}}}{hT^{\text{SG\_ sandwich}}} - \frac{I^{solid\ glass}}{hT^{solid\ glass}} \right) \qquad (8)$$

This conventional SANS reduction has been refined by *Brûlet et al.* [5] to account for large angle corrections, beyond which the assumption $cos\ \theta \approx 1$ does not hold (typically for sample-detector distances ≤ 2m), which otherwise affect the high q scattering data. Further, the authors introduced an improvement over eq. (8) for the reduction of the scattering by a sample inside a container (eq. 17 in their paper), which becomes

[1] In limiting cases where the channel thickness is very small compared to the overall device thickness, or when the channel area fraction is very small ($t \gg h$ or $t \gg 1-\varphi$), then

$$I^{empty} \approx K_{abs} \frac{I^t}{tT^t} \qquad (4)$$

The effects of this simplification are illustrated as

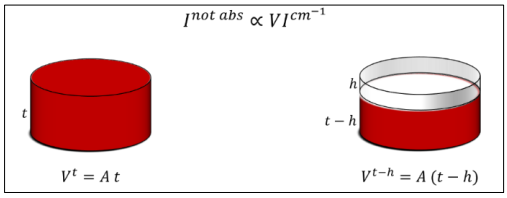

Scheme S3: Comparison between the illuminated volume of a sample cell, ignoring (left) and considering (right) the volume occupied by microchannels of small volume fraction.

Taking t = 4.63 mm and h = 0.25 mm,

$$\frac{V^{t-h}}{V^t} = \frac{t-h}{t} = 0.9946$$

and the scattering and transmission of the empty microdevice with and without subtracting the volume of the microchannels is effectively identical, and can be ignored yielding a minute correction, $I^{not\ abs} = 0.9946 V^t I^{cm^{-1}}$.[1]

particularly significant for strongly scattering containers (such as those used in high pressure or shear studies). Under the current experimental conditions, we restrict ourselves to the traditional reduction given in eq. (8), which we validate experimentally against standard measurements with hellma cells.

For strongly scattering systems, i.e. if $I^{SG\_sandwich} \gg I^{solid\ glass}$, eq. (6) can be simplified as:

$$I^{total} \approx (1-\varphi) I^{\mathrm{SG\_sandwich}} \qquad (9)$$

The *proposed data reduction* method is divided in two phases: (i) the subtraction of the bulk glass contribution, illustrated in Scheme 5, and (ii) the reduction and calibration as a standard "sandwich" cell.

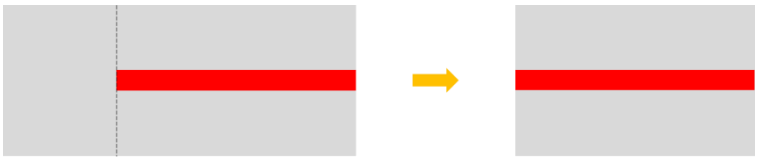

Scheme S4: Step (i) of data reduction: subtraction of the scattering signal from the solid glass.

The glass and sample transmissions can be calculated from eq. (2) and (5). The scattering signal is calculated from eq. (7), thus taking the raw scattering pattern of total device with sample, I^{total}, subtracting $\varphi I^{solid\ glass}$ where φ=0.6(6), and divided by 1-φ = 0.3(3), the area fraction of the sample.

The second step (ii), illustrated below, involves taking the thus obtained standard cell, i.e. "sandwich", scattering intensity $I^{\mathrm{SG\_sandwich}}$ and carrying out a standard data reduction and calibration to obtain I^{sample}, given by eq. (8), using the glass transmission obtained from eq. (2).

Scheme S5: Step (ii) of data reduction: standard cell subtraction and sample data calibration to absolute units.

Given the device geometry employed in this paper, the data reduction was carried out as follows:

1. The transmission of the glass (without channels) is taken to be that of the experimentally measured (solid glass + sample glass sandwich), since their difference is ≈0.3%:

$$T^{solid\ glass} \approx T^{empty} \qquad (10)$$

2. The scattering intensity of the solid glass is the same of the one that is experimentally measured as an empty glass sandwich, since their difference is ≈0.05%

$$I^{solid\ glass} \approx I^{empty} \qquad (11)$$

Then, the calibrated scattering intensity of the sample, from eq. (8), can be simplified as follows:

$$I^{sample} = K_{abs}\left(\frac{I^{total} - \varphi I^{empty}}{1-\varphi} - \frac{I^{empty}}{hT^{\mathrm{SG\_sandwich}}}\right) \qquad (12)$$

where the transmission of the glass+sample sandwich is:

$$T^{SG\_sandwich} = \frac{T^{measured} - \varphi T^{empty}}{1-\varphi} \qquad (13)$$

II. Scattering of H_2O:D_2O at different ratio and sample thickness

This approach was validated using solutions of H_2O/D_2O in the microdevice (h=0.25 mm) and compared to references in standard quartz cuvettes of varying neutron pathlength (0.5, 1 and 2 mm). This validation is non-trivial as the incoherent scattering intensity of water (H_2O) depends on thickness due to the combined effects of multiple scattering and inelasticity (discussed, for instance, by May *et al.* [6]. These results are shown in Figure S1 and converge at the pure D_2O signal, enabling us to calibrate H_2O:D_2O content from scattering data, at various sample thicknesses.

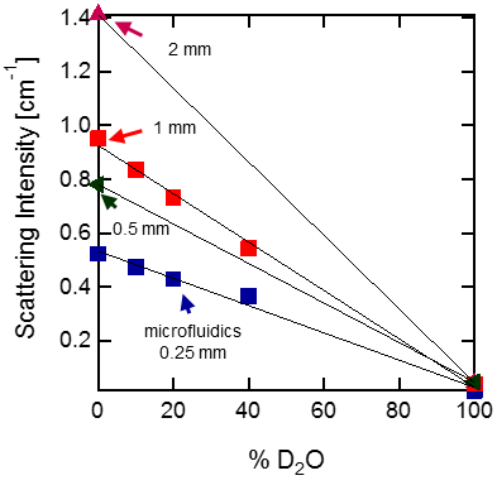

Figure S1: Benchmark of the microfluidic data (h=0.25 mm) with standard Hellma cuvettes of a different pathlength (0.5, 1 and 2 mm) filled with isotopic mixtures of water and heavy water.

III. Effect of neutron beam shape on RTD

The neutron beam shape is generally defined by Cd diaphragm of prescribed geometry. Typically, these diaphragms are circular with a diameter of the order of 12 mm. While smaller diaphragms can be machined and utilized, down to sub mm dimensions, the neutron flux suffers nearly proportionally with the decrease in area. We have therefore opted to over-illuminate several microchannels and explicitly compute the ensuing compositional dispersion. Relevant RTDs were computed for diaphragms of various shapes and constant area (and thus neutron flux). In Figure S2, the RTD calculates for 20 channels illuminated by a circular beam of 12 mm in diameter is calculated with flow rate 0.1 ml/min. The individual RTDs per channel were computed and the overall, envelope RTD calculated by weighting by the illuminated area of each channel.

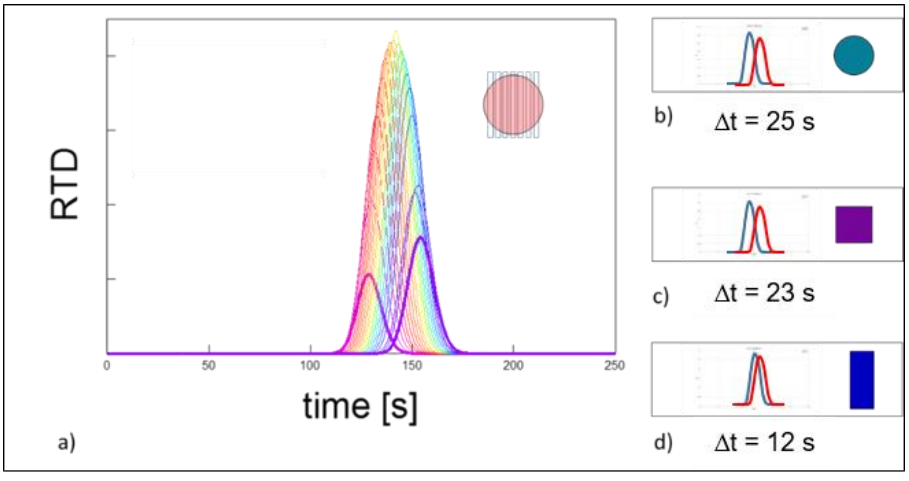

Figure S2: Effects of overillumination on (a) RTD distribution. Effect of the beam shape (b, c, d) at a fixed illuminated area, on the RTD of the first and last channels that are illuminated by the beam.

In Figure S2b-d, only the RTDs corresponding to the first and last illuminated channels for a b) circular, c) square and d) rectangular beam shape, of identical area, are plotted. Evidently, narrower RTDs are obtained by selecting a rectangular beam shapes with the long axis parallel to the main channel direction.

IV. Step response

The SANS step response was experimentally measured and the RTD calculated for different flowrates that are typically used in microfluidics, from 0.05 ml/min to 0.2 ml/min. The step profile of concentration is obtained by filling the device with a H_2O:D_2O ratio of 95:5 and then swapping the two flowrates. The RTD is computed from the derivative of the measured step of the average total scattering response. The transmission is plotted to conform the accuracy of the measurements. As expected, an increase in flow rate causes a narrowing of the RTD, thus suggesting that higher flowrates help mitigate the drawbacks of composition dispersion gauged by the residence time distribution. The maximum feasible rate is, however, limited by the total sample volume consumption, the requirement of full mixing within the device, and by material requirements (pressure build up and device leakage, and/or fluctuations).

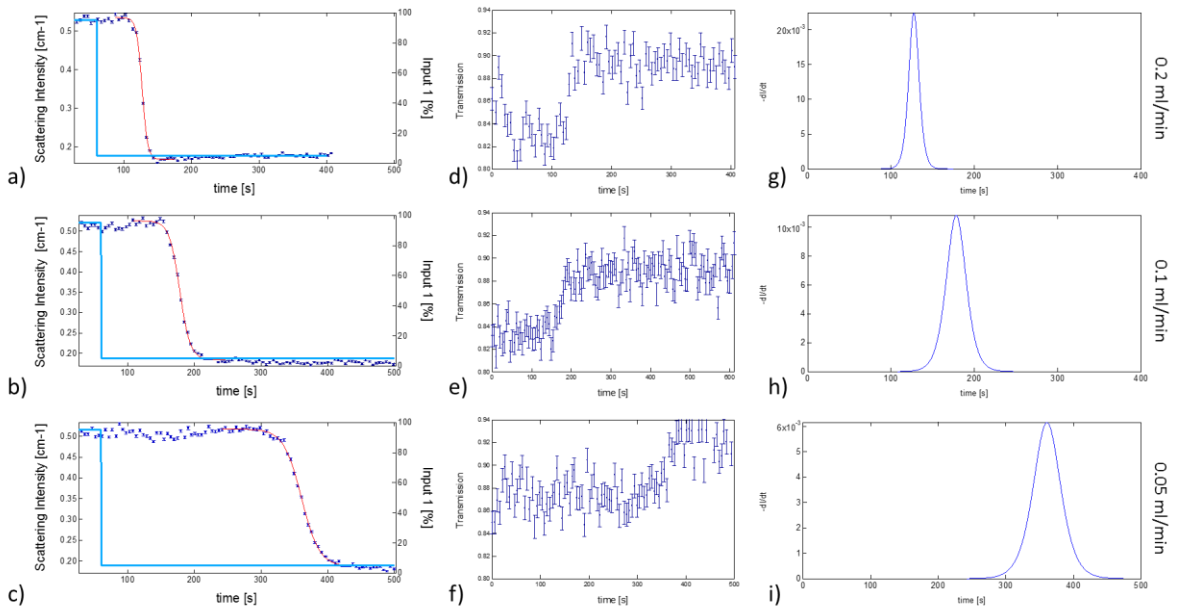

Figure S3: Experimental SANS step response measured for total flow-rate of 0.2ml/min, 0.1ml/min, 0.05ml/min. a,b,c) SANS response (blue), imposed flow profile (light blue), fit (red). d,e,f) Calculated transmission. g,h,i) Derivative of the SANS step response. All data obtained for H_2O:D_2O swapping from a ratio of 95:5 to 5:95.

V. Contrast variation of Ludox in discrete 1mm Hellma cells.

For validation of the microfluidic CV data, we report the I(q) curves of the contrast variation of Ludox in standard hellma cells.

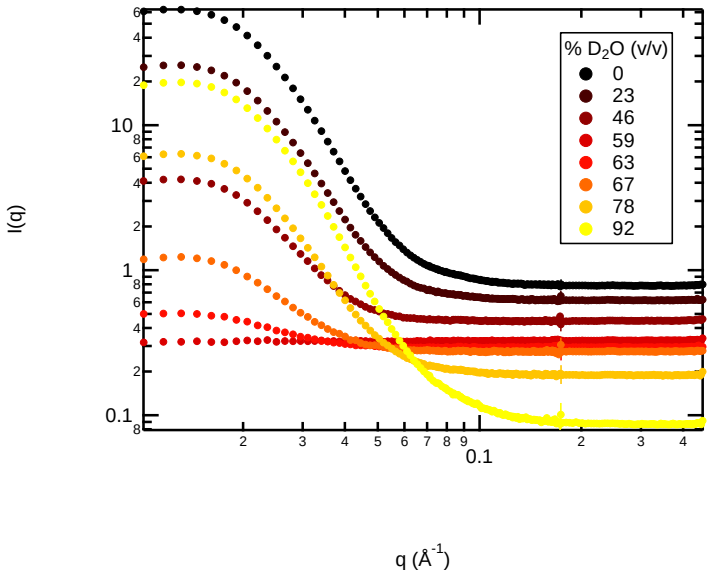

Figure S4: Contrast variation of Ludox 4.6% w/w in standard 1 mm hellma cells at different ratios of [D_2O]:[H_2O] (v/v), indicated in the figure.

VI. Fit of micellar SDS in aqueous solution

Each 2D scattering pattern was radially averaged and calibrated to obtain *I(q)*, and fitted using SasView, by the means of the EllipsoidModel for the form factor and HayterMSAStructure for the structure factor [7]. The known parameters were fixed: charge (42.526), dielconst (71.31), saltconc (0.001 M), temperature (298 K), following Hammouda *J. Res. Nat. Inst. Stand. Tech.* **118**, 151-167 (2013). The "scale factor", SLD of the solvent and background B were allowed to vary. The same model was used to fit all scattering curves measured with varying isotopic aqueous composition, given by (from SasView user documentation)

$$P(q,\alpha) = \frac{scale}{V} f^2(\boldsymbol{q}) + bkg \qquad (14)$$

where *scale* is the scale factor, V the volume of the ellipsoid, and *bkg* is the scattering background and:

$$f(\boldsymbol{q}) = \frac{3(\Delta\rho)V\,[sin\left(qr\left(R_p, R_e, \alpha\right)\right) - qrcos\left(qr\left(R_p, R_e, \alpha\right)\right)]}{[qr\left(R_p, R_e, \alpha\right)]^3} \qquad (15)$$

where $\Delta\rho$ is the contrast, R_p the polar radius along the rotational axis, R_e the equatorial radius, and r is:

$$r\left(R_p, R_e, \alpha\right) = \left[{R_e}^2 sin^2\alpha + {R_p}^2 cos^2\alpha\right]^{1/2} \qquad (16)$$

where α is the angle between the axis of the ellipsoid and the scattering vector *q*.

VII. Contrast Variation of F127

The microflow contrast variation has been performed on Pluronics F127, at several concentrations in isotopic aqueous solutions, at *F*=0.1 ml/min, *N*=120 and Δt =5s or 10s. F127 is a triblock copolymer composed of PEO/PPO/PEO whose SLDs ate ρ_{PEO}= 0.572 10^{-6} Å^{-2} and ρ_{PPO}=0.347 10^{-6} Å^{-2}. Similarly to the case of SDS, the contrast match point is close to pure H_2O. Selected experimental results are plotted for 3% and 2% w/v F127 in isotopic mixtures.

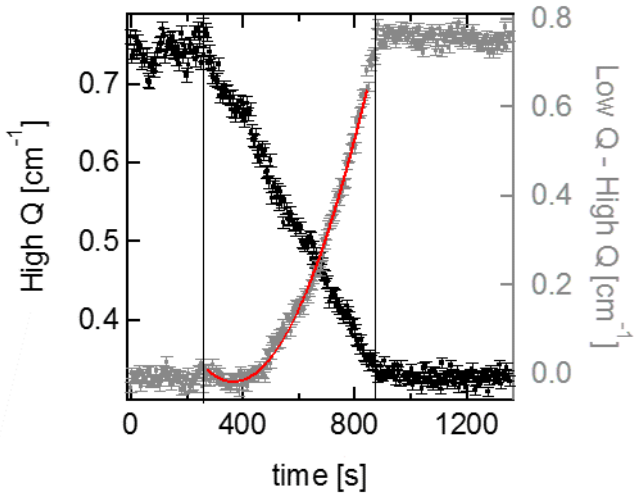

Figure S5: Contrast variation in microflow-SANS of Pluronics F127 3% (w/v) from 95% H_2O to 5% H_2O

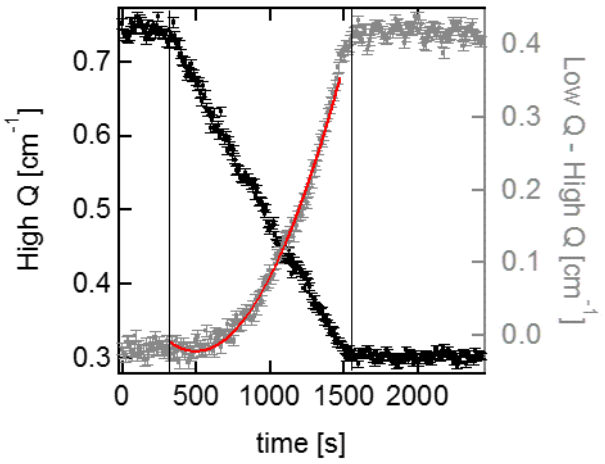

Figure S6: Contrast variation in microflow-SANS of Pluronics F127 2% (w/v), with Δt=10s.

For completion, the experiment was also benchmarked against the standard discrete approach in 1 mm quartz Hellma cells, and the results are shown in Fig S7. The contrast match point was found to be 14.5% v/v D_2O in the discrete approach and 14.34% v/v by microflow-SANS.

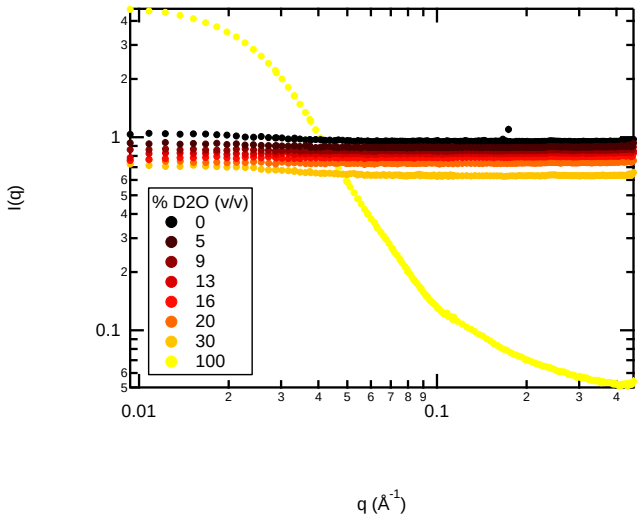

Figure S7: Hellma contrast variation of 2% F127 w/v at the aqueous isotopic compositions shown in the legend.

References

[1] J. T. Cabral, S. D. Hudson, C. Harrison, and J. F. Douglas, "Frontal Photopolymerization for Microfluidic Applications", *Langmuir* **20**, 1 0020 (2004).

[2] C. G. Lopez, T. Watanabe, A. Martel, L. Porcar, and J. T. Cabral "Microfluidic-SANS: flow processing of complex fluids" *Sci. Rep.* **5**, 7727 (2015)

[3] HP Martin et al., "Microfluidic processing of concentrated surfactant mixtures: online SAXS, microscopy and rheology" *Soft Matter* **12**, 1750-1758 (2016)

[4] A. S. Poulos et al., "Microfluidic SAXS study of lamellar and multilamellar vesicle phases of linear sodium alkylbenzene sulfonate surfactant with intrinsic isomeric distribution" *Langmuir* **32** (23), 5852–5861 (2016)

[5] A. Brûlet, D. Lairez, A. Lapp and J. P. Cotton "Improvement of data treatment in small-angle neutron scattering" *J. Appl. Cryst.* **40**, 165–177 (2007)

[6] R. P. May, K. Ibel and J. Haas "The forward scattering of cold neutrons by mixtures of light and heavy water" *J. Appl. Cryst.* 15, 15-19 (1982).

[7[SAS view

[8] B. Hammouda "Temperature Effect on the Nanostructure of SDS Micelles in Water" *J. Res. Nat. Inst. Stand. Tech.* **118**, 151-167 (2013).